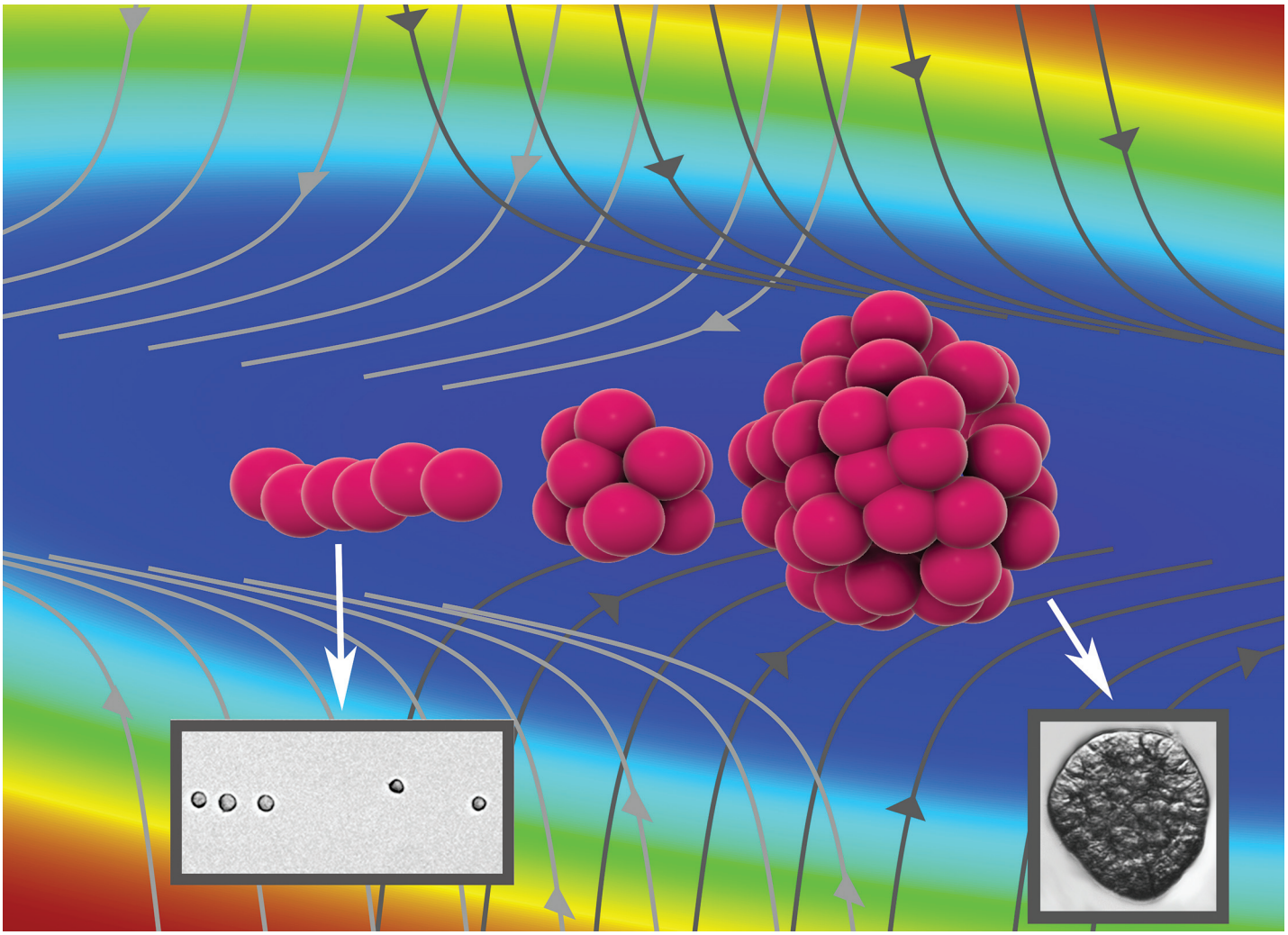

Highlighting research from Ahu Arslan-Yildiz and co-workers, Biomimetics Research Group at Izmir Institute of Technology (IZTECH).

Scaffold-free three-dimensional cell culturing using magnetic levitation

Three-dimensional (3D) cell culture has emerged as a pioneering methodology and is increasingly utilized for tissue engineering, 3D bioprinting, cancer model studies and drug development. Magnetic levitation methodology is a newly developed, innovative technique enabling the formation of scaffold-free 3D cell culture and cellular assembly by favoring cell–cell, cell–ECM interactions in the presence of paramagnetic gadolinium agents. Herein, the magnetic levitation technique has been utilized to manipulate and orientate living cells in 3D to form complex cellular structures.

As featured in:

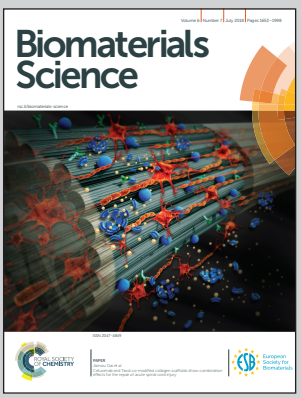

See Ahu Arslan-Yildiz *et al.*, *Biomater. Sci.*, 2018, **6**, 1745.

ROYAL SOCIETY OF CHEMISTRY

rsc.li/biomaterials-science

Registered charity number: 207890

Biomaterials Science

PAPER

View Article Online
View Journal | View Issue

Cite this: *Biomater. Sci.*, 2018, **6**, 1745

Scaffold-free three-dimensional cell culturing using magnetic levitation

Esra Türker, Nida Demirçak and Ahu Arslan-Yildiz *

Three-dimensional (3D) cell culture has emerged as a pioneering methodology and is increasingly utilized for tissue engineering, 3D bioprinting, cancer model studies and drug development studies. The 3D cell culture methodology provides artificial and functional cellular constructs serving as a modular playground prior to animal model studies, which saves substantial efforts, time and experimental costs. The major drawback of current 3D cell culture methods is their dependency on biocompatible scaffolds, which often require tedious syntheses and fabrication steps. Herein, we report an easy-to-use methodology for the formation of scaffold-free 3D cell culture and cellular assembly *via* magnetic levitation in the presence of paramagnetic agents. To paramagnetize the cell culture environment, three different Gadolinium(III) chelates were utilized, which led to levitation and assembly of cells at a certain levitation height. The assembly and close interaction of cells at the levitation height where the magnetic force was equilibrated with gravitational force triggered the formation of complex 3D cellular structures. It was shown that Gd(III) chelates provided an optimal levitation that induced intercellular interactions in scaffold-free format without compromising cell viability. NIH 3T3 mouse fibroblasts and HCC827 non-small-cell lung cancer cells were evaluated *via* the magnetic levitation system, and the formation of 3D cell culture models was validated for both cell lines. Hereby, the developed magnetic levitation system holds promises for complex cellular assemblies and 3D cell culture studies.

Received 31st January 2018,
Accepted 12th April 2018

DOI: 10.1039/c8bm00122g

rsc.li/biomaterials-science

Introduction

Through development of three-dimensional (3D) cell culturing techniques, a variety of systems have been reported for different cellular applications such as drug screening,[1–4] cancer studies,[5–8] protein expression studies[9–12] and artificial tissue/organ studies.[13–16] Reliable techniques and models are required for real-time monitoring of cellular responses, and 3D cell culture has been shown as the most promising model since it exhibits many features of complex *in vivo* systems. A variety of 3D cell culturing methodologies[12,17,18] and materials[19–21] have been reported during the last decade, showing the ability of 3D systems to overcome the problems arising from traditional two dimensional (2D) cell culture system and substrates.[22,23] The most commonly used materials are (i) synthetic materials such as polymers,[24–26] (ii) natural materials such as collagen, fibrinogen, and gelatin[27–29] or (iii) synthetic/natural material hybrids.[30–34] The most important contribution of these hybrid materials is the mimicking of real extracellular matrix (ECM) environment while providing more robust and stable scaffolds. Although the diversity of materials and scaffold fabrication methods is helpful, it hardly provides real ECM microenvironment successfully.

Besides, different approaches[35–38] involving spheroid formation provide scaffold-free environment for 3D cell culturing; despite their success in the formation of 3D cell cultures in a scaffold-free environment, these systems have some limitations, and some of them do not allow long-term cellular studies. Although new methodologies and materials have been developed to improve the 3D cell culture efficiencies, most attempts do not meet the requirements of practical and clinical applications.

Herein, we present a simple, straightforward and powerful technology based on the magnetic levitation technique for scaffold-free formation of 3D cell cultures. The reported technique is an alternative to both scaffold-based and scaffold-free 3D cell culture systems. This new technology is based on magnetic levitation of cells, which assemble into a 3D cell culture while secreting their own ECM. The magnetic levitation platform creates a suitable microenvironment for the cells, which retain their cellular activities while creating 3D organoid structures.

Application of magnetic forces principle, where magnetic force arise against gravitational force, through magnetic levitation for biological systems has been studied quite recently.[12,39–42] For

Department of Bioengineering, Izmir Institute of Technology (IZTECH), 35430 Izmir, Turkey. E-mail: ahuarslan@iyte.edu.tr

example, hydrogels containing gold and iron oxide magnetic nanoparticles have been used as a helping tool to levitate and to produce 3D cell cultures.[12] In another study, to magnetize the cells, cationic polyelectrolyte-coated magnetic nanoparticles attracting negatively charged cells, were employed for planar cell sheet and 3D multicellular spheroid formation.[41] A magnetic levitation platform is also utilized for the formation of a 3D cell culture while using agarose gel as a scaffold material.[39]

Herein, we report the utilization of various paramagnetic agents, namely, gadolinium(III) chelates for the formation of scaffold-free 3D cell cultures by using a newly developed magnetic levitation platform. The magnetic levitation platform enables and favors cell–cell interactions and creates stimuli for the 3D cell culture formation due to the alignment of magnetically levitated cells at the same level under microgravity conditions (Fig. 1A). This developed technology provides an optimum microenvironment for the cells to assemble into a 3D cell culture while secreting the required ECM molecules of their own. Thus, the developed system allows us to confirm and then evaluate the formation of a 3D cell culture in a scaffold-free format.

Materials/methods

Fabrication of magnetic levitation setup

N52 grade custom-made Neodymium (NdFeB) magnets (K&J Magnetics) ~0.4 T with a size of 2.0 × 5.0 × 50 mm were used for the fabrication of the magnetic levitation setup. Mirrors and magnets were assembled (Fig. 1B and C) using polymethylmethacrylate (PMMA) holders, which were laser cut from 1.5 mm thick PMMA sheets *via* Versa Laser VLS 2.30 (Universal Laser). Borosilicate capillary tubes (VitroCom) with a size of 1.0 × 1.0 × 50 mm were inserted into the magnetic levitation setup before each experiment. Mirrors were placed at 45° angles (Fig. 1B and C) to visualize the capillary channel and its content through an inverted microscope (Zeiss Observer Z1).

Cell lines and cell culture

NIH 3T3 mouse fibroblast cells and HCC827 non-small-cell lung cancer cells were cultured respectively in high glucose DMEM (GIBCO, ThermoFischer Scientific) containing L-glutamine and RPMI medium (GIBCO, ThermoFischer

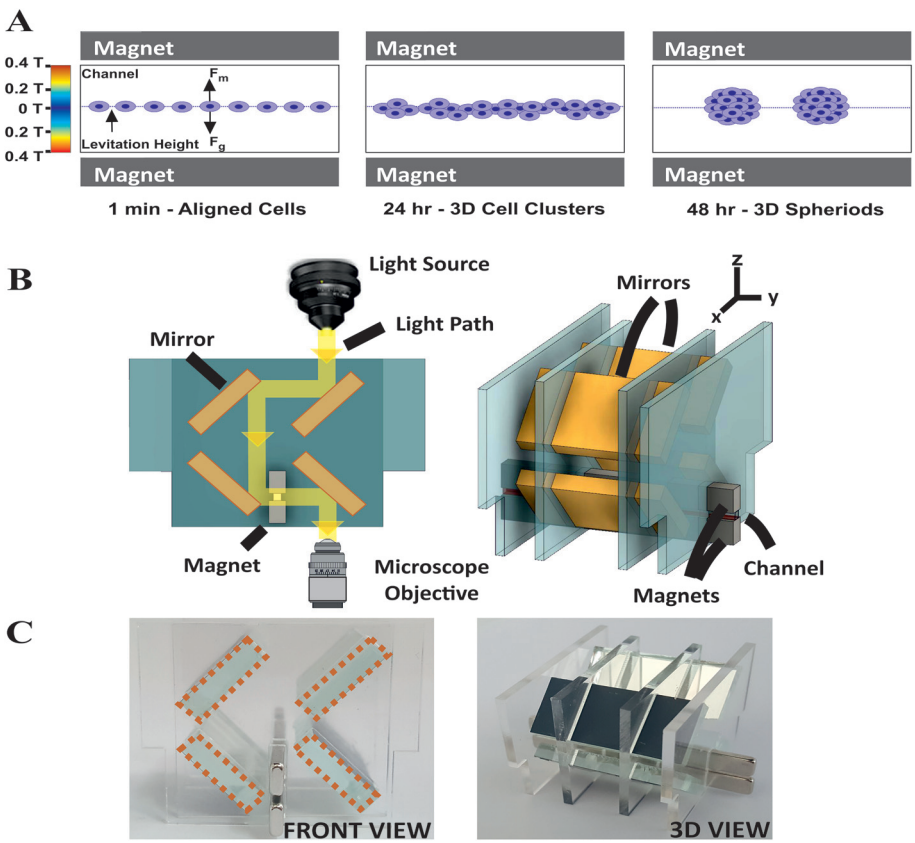

Fig. 1 Working principles and design of magnetic levitation platform. (A) Schematic representation of magnetic levitation technology and 3D cell culture formation *via* magnetic levitation. Magnetic field gradient inside the capillary channel varies from 0.4 T to 0 T when the two NdFeB magnets are placed with their same poles facing each other. Magnetic and gravitational forces guide cells to assemble at the levitation height (*z*). Aligned cells are forced to interact with each other, which leads to 3D cell culture formation. (B) 2D and 3D designs of 4-mirror-based magnetic levitation setups. (C) Front and 3D view of the magnetic levitation setup after assembly of all components: mirrors, capillary glass channel, NdFeB magnets assembled by transparent PMMA holders.

Scientific), supplemented with 10% FBS (GIBCO, ThermoFischer Scientific), 50 units per ml penicillin, and 50 units per ml streptomycin. The cells were cultured up to ~90% confluency in a humidified environment (5% CO_2, 37 °C); the harvested cells were used further for long-term cell culture and magnetic levitation studies.

System calibration, modeling studies and image processing

The system calibration study was carried out *via* fluorescent-featured polyethylene beads (Cospheric LLC). The densities of the polyethylene beads were 1.02 ± 0.005, 1.13 ± 0.005, 1.09 ± 0.005, 1.08 ± 0.005, 1.06 ± 0.005 and 1.04 ± 0.005 g cc^{-1}, and these beads were suspended in DMEM at varied concentrations (0/30/50/100/200 mM) of Gd(III) chelate solutions. Gd(III) chelates, namely, Gadobutrol (Gadovist, Bayer), Gadodiamide (Omniscan, GE) and Gadoteric Acid (Dotarem, Guerbet) were utilized as paramagnetic agents, and their levitation capabilities were investigated. The beads were loaded into capillary tubes, and the capillary tubes were placed between two magnets and levitated. Image analysis was done *via* the ImageJ software (NIH). According to the levitation heights of the beads, a density *versus* height graph was plotted to obtain the standard curve for density characteristics. The levitation height is given by "*z*", which represents the vertical position of the object inside the 1 mm channel.

To analyze the effect of paramagnetic Gd(III) chelates on cells, 2D cultured cells were resuspended in DMEM containing different Gd(III) chelates in varied concentrations (0/30/50/100/200) mM. Later, levitation heights and densities of the cells were evaluated for each Gd(III) chelate through previously obtained calibration curves.

Optimization of Gd(III) chelates for magnetic levitation application and viability determination

To investigate the levitation capability and toxic behavior of Gd(III) chelates, first, NIH 3T3 cells were investigated as a model system. The cells were seeded in a 96-well plate with a starting number of 1×10^3 cells per well. Varied concentrations of Gd(III) chelates (0/30/50/100/200 mM) were added in the cells, and the cells were incubated for 7 days. The culture medium and Gd(III) chelate solutions were replenished every 2 d.

For Live/Dead assay experiments, CytoCalcein™ Green and Propidium Iodide (PI) dyes (AATBioquest) were used in equal proportions and added into the assay buffer solution. Cells were stained with the dye-loading solution at 37 °C for 30 min. Then, viability analysis was performed using a fluorescence microscope (Zeiss Observer Z1); image analysis and cell counting were conducted *via* the ImageJ software (NIH). MTT assay was conducted to quantify the cell viability in long term (7 days). The MTT reagent thiazolyl blue tetrazolium bromide (Sigma Aldrich) was added (5 mg mL^{-1}), and the cells were incubated for 2–4 h. After incubation, live cells reduced tetrazolium to formazan and dissolved by solubilizing in reagent DMSO. The resulting dye was measured by a Multiskan™ GO Microplate Spectrophotometer (ThermoFischer Scientific). All the data from varied concentrations, including those from the control group, were collected and evaluated from at least 4 independent samples.

3D Cell culture *via* magnetic levitation

Components of the magnetic levitation setup were UV sterilized at least 30 min prior to cell culture studies. The cell lines were expanded and cultured in 25–175 cm^2 tissue culture plates. The cells were harvested at ~90% confluency and resuspended in 50 mM Gadobutrol (Gadovist) containing a cell culture medium (DMEM supplemented with 10% FBS and Pen/Strep). Next, the cell culture mixture was loaded into 1 mm square glass capillary tubes (VitroCom) and cultured in 5% CO_2 at 37 °C up to 7 days for long-term 3D cell culture studies. At varied time intervals, 3D cell culture formation was evaluated using light microscope snapshot images.

The contents in the capillary tubes were taken into 96-well plates after certain incubation time frames to collect 3D cell structures for further viability and Live/Dead analysis. Cell proliferation and viability for the 3D levitated cell cultures were evaluated through Trypan Blue and Live/Dead assay. Each time point, concentration or other variables are given by mean values of at least three independent samples.

Results and discussion

Design and development of magnetic levitation platform

The basic principle of the magnetic levitation technology is given in Fig. 1A. Briefly, cells are suspended in capillary channel, and the cell suspension medium is paramagnetized by Gd(III) chelates (*i.e.*, Gadobutrol, Gadoteric acid, and Gadodiamide). The cells are levitated to a certain height, named as levitation height (*z*) or equilibrium height, upon insertion of the channel into the magnetic levitation platform. In a paramagnetized environment, the cells are forced to migrate from a higher magnetic field region to a lower magnetic field region till they reach the levitation height. At the levitation height, the cells assemble due to a balance of magnetic, gravitational and buoyancy forces[39] This assembly and close interaction of cells triggers the 3D cell culture formation (Fig. 1A).

In this report, a custom magnetic levitation setup was developed and improved based on the previously used setup.[43] The design of the magnetic levitation setup (Fig. 1B) was done using the Autodesk Fusion software. As shown in Fig. 1C, all components of the setup, *i.e.*, mirrors, magnets and glass capillary channel were assembled by using laser-cut PMMA sheets. Although the previously used setup was an easy-to-use system,[43] it had limitations in terms of visibility that required fine alignment of components, which has certain dimensions. Especially, alignment of the light path is required when regular mirrors are used. The light path was improved, and 4-mirror-based design was developed to improve the visibility and image quality. With this improved setup, no adjustment was required for the light path, and it was compatible with varied mirror sizes and shapes. Most importantly, it could be used in varied microscope types.

Light path, focusing of cells and visibility are improved and therefore, monitoring the cell characteristics, cell behavior, and cellular properties such as density profiles and 3D cell culture formation are substantially facilitated by this device. Herein, cells were easily focused and visualized inside the capillary channel while minimizing the background problem. The advantages of the developed system include (i) simple component requirements, (ii) easy assembly and fabrication procedure, (iii) autoclavable, reusable and disposable design, which is especially useful for cell culture studies, (iv) compatibility with varied microscopy setups, (v) improved light path and visibility, and (vi) real time monitoring and analysis of 3D cell culture such as investigation of spheroid formation and density profiles.

Optimization of magnetic levitation platform and Gd(III) chelates

Gd(III) chelates have long been used as phase contrast agents in MRI applications.[44,45] However, the use of Gd(III) chelates in magnetic levitation is quite a new concept for 3D cell culture.[43] Herein, the levitation capabilities of three different Gd(III) chelates and their effects on 3D cell culture were investigated. Three commercially available Gd(III) chelates Gadobutrol (Gadovist, Bayer), Gadodiamide (Omniscan, GE) and Gadoteric Acid (Dotarem, Guerbet) were chosen based on their ionic/non-ionic, macrocyclic/linear chain characteristics (Fig. 2A). They were all utilized to paramagnetize the cell

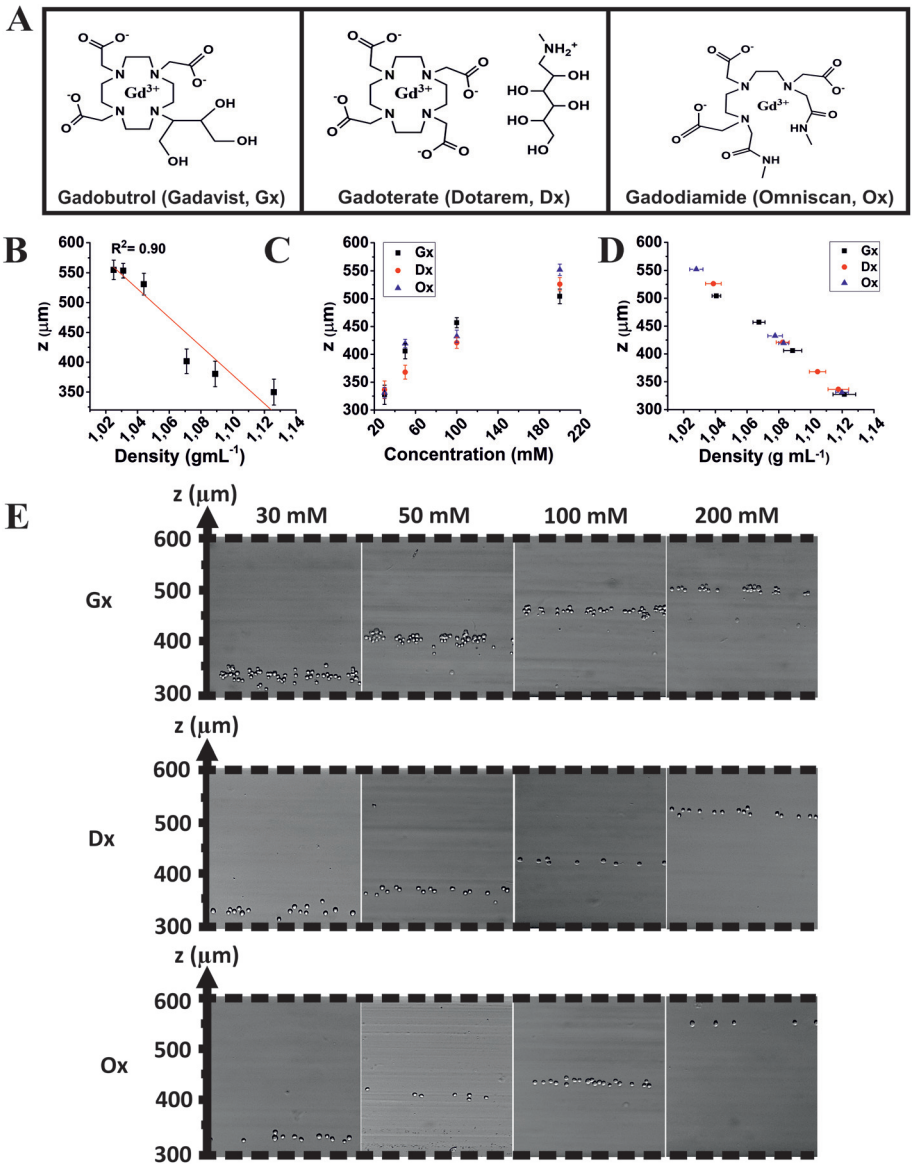

Fig. 2 Evaluation of levitation height (*z*) and density profiles through magnetic levitation. (A) Standard curve for PE bead density against levitation height; linear curve fitting gives the standard function for the corresponding curve. (B, D) Levitation height profiles of single NIH 3T3 cells under 30/50/100/200 mM Gd concentrations. (C) Single cell density profiles calculated through standard function of linear fitting. Gd(III) chelates were named as Gx (Gadovist/Gadobutrol), Dx (Dotarem/Gadoteric acid) and Ox (Omniscan/Gadodiamide).

culture medium to levitate the cells under scaffold-free conditions.

To characterize the imaging capability of the magnetic levitation setup, polyethylene (PE) density marker beads were used. PE beads having varied densities, such as 1.02, 1.04, 1.06, 1.08, 1.09 and 1.13 g cc^{-1}, were utilized as standards to calibrate density gradient in the capillary column under 0/30/50/100/200 mM Gd concentrations. Fig. 2B shows an almost linear and inverse relation of density with the levitation height. A linear fitting curve represents a standard function to evaluate unknown density profiles of cells and cell spheroids. Levitation height profiles of the NIH 3T3 cells (Fig. 2C and E) were calculated through this standard curve. NIH 3T3 cells were levitated in cell media containing varied concentrations (0/30/50/100/200 mM) of three different paramagnetic Gd(III) chelates (Fig. 2C and E). The cells reached equilibrium in 5 min, where there was a balance between magnetic and gravitational forces. At equilibrium height, the magnetic and gravitational forces equilibrated with the buoyancy forces acting on the levitating object. All measurements were completed when the cells reached the equilibrium height. As expected, the levitation height of the cells increased inside the capillary channel from 325 μm position to 500–550 μm position with an increase in Gd concentration from 30 mM to 200 mM (Fig. 2D), which showed the levitation capability of the chosen Gd(III) chelates.

Evaluating cell viability

To investigate the impact of various Gd(III) chelates in terms of chemical content and structure, cell viability and toxicity were investigated for long term culture of NIH 3T3 cells. The three different gadolinium agents (Fig. 2A) Gadobutrol (Gadovist, Gx), Gadoteric acid (Dotarem, Dx) and Gadodiamide (Omniscan, Ox) were tested to interpret their toxicities as well as their effects on cell viability, which were analyzed by both MTT and Live/Dead assays. The medium containing Gadobutrol exhibited maximum cell viability when compared with media containing Gadoteric acid and Gadodiamide. As shown in Fig. 3 and 4, MTT and Live/Dead analysis results both showed that Gadobutrol provided the best conditions with the increasing Gd concentrations. High cell viability was observed up to 100 mM Gd concentrations when Gadobutrol was supplied into the cell culture medium. Also, good cell viability was observed at 200 mM, which was the highest Gd concentration used for the optimization studies. Considerable viability was observed when 30 and 50 mM Gadoteric acid solutions were supplied; however, above these concentrations, cell viability was not observed. Last, an increase in Gd concentrations caused cell death even at very low Gd concentrations such as 30 mM for Gadodiamide.

The previous pharmacovigilance studies conducted for gadolinium-based contrast agents (GBCAs) revealed that the

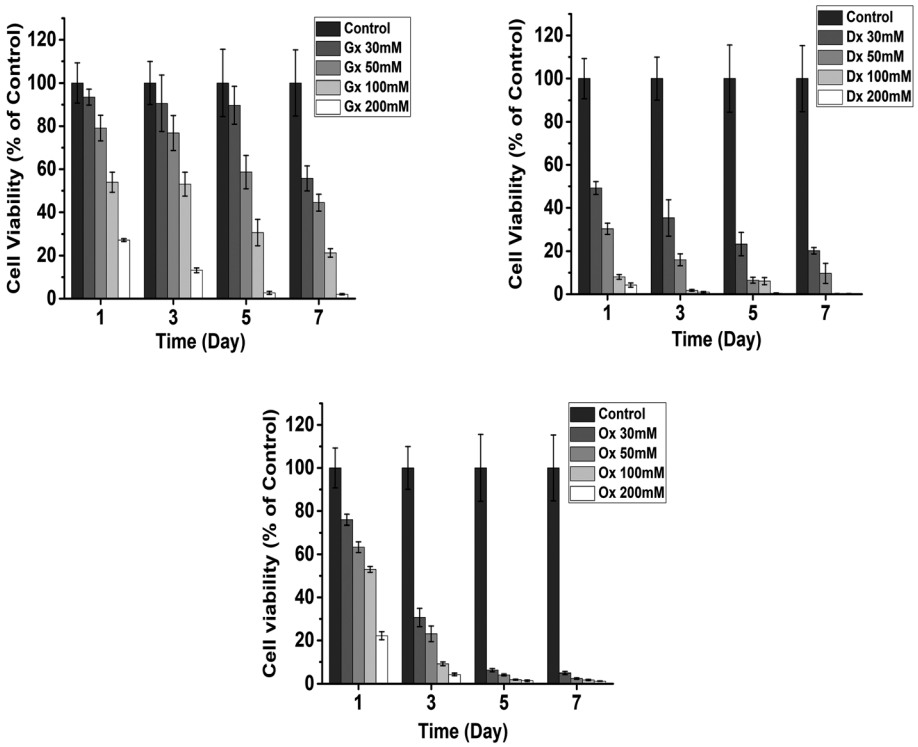

Fig. 3 Effect of Gd(III) chelates on cell viability. Gd(III) chelates were named as Gx (Gadovist/Gadobutrol), Dx (Dotarem/Gadoteric acid) and Ox (Omniscan/Gadodiamide). Cell viability was analyzed by MTT assay for long-term culturing. NIH 3T3 cells were cultured under 0/30/50/100/200 mM Gd concentrations.

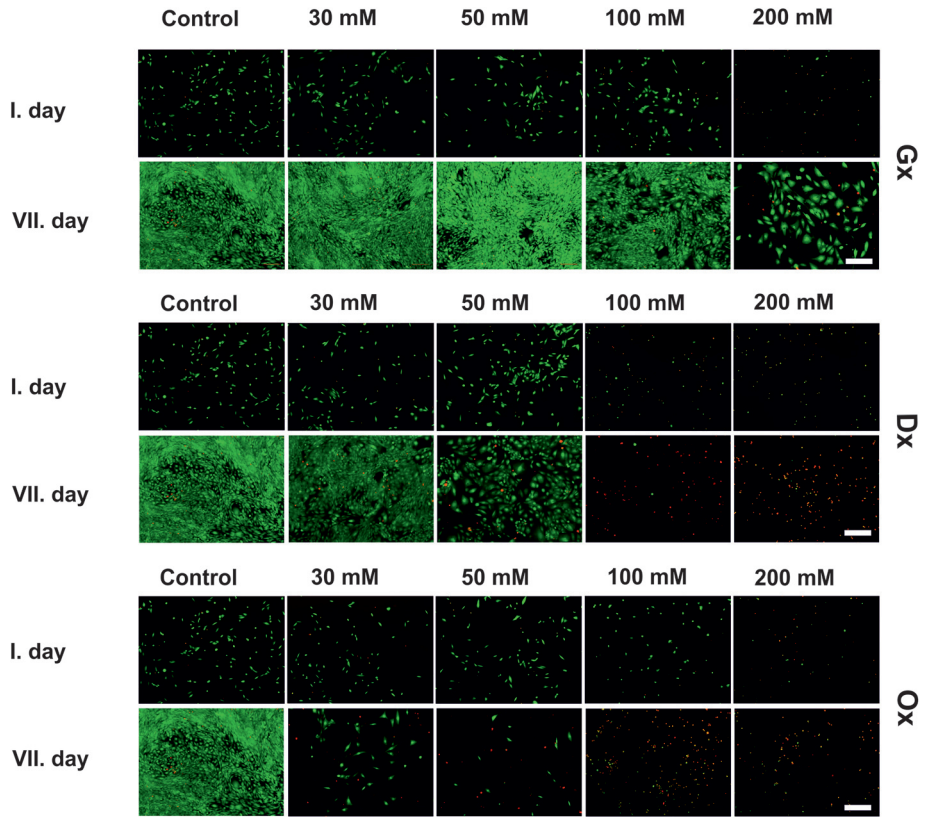

Fig. 4 Cell viability *via* Live/Dead analysis. Comparison of effect of Gd(III) chelates on cell viability. NIH 3T3 cells were cultured and analyzed in standard 2D platform under 0/30/50/100/200 mM Gd concentrations. Scale bar: 100 μm. Gd(III) chelates were named as Gx (Gadovist/Gadobutrol), Dx (Dotarem/Gadoteric acid) and Ox (Omniscan/Gadodiamide).

release of free gadolinium ion is the main reason of the toxic effect, and the release of gadolinium ions has been linked to stability and half-life of the chelates in physiological conditions.[46] The percent release of Gadobutrol and Gadoteric acid have been reported as 0.007 per day, which is nearly 22-fold lesser than that of Gadodiamide, which exhibits the lowest cell viability. The major reason of the higher toxicity of Gadodiamide is fast dissociation of its ligand, releasing gadolinium ions due to its linear chain ligand structure. The half-life, $t_{1/2}$, of Gadodiamide has been deduced as 0.01 hours, which is ~700- and ~2300-fold faster than those of Gadoteric acid and Gadobutrol, respectively; this suggests that Gadodiamide shows fast dissociation period as compared to other paramagnetic agents. Gadoteric acid and Gadobutrol have macrocyclic ligand structures, and they exhibit better cell viabilities with respect to Gadodiamide. However, Gadoteric acid causes relatively higher toxicity and lower cell viability in the 50–200 μM range as compared to Gadobutrol. As discussed previously, $t_{1/2}$ of Gadobutrol is about 23 hours, which is three times longer than that of Gadoteric acid, resulting in lower release of gadolinium ion. These results suggest that the ligand structure induces strong association of gadolinium ion thereby lessening the release of free gadolinium and lowering the toxic effect.

Magnetic levitation of cells and 3D cell culture formation

NIH 3T3 and HCC 827 cells were used as models to evaluate the ability of the magnetic levitation setup for 3D cell culture formation. First, the cells were cultured in 2D to reach the desired confluence. Later, the cells were resuspended in cell culture medium supplied with paramagnetic agent, and they were injected into a capillary channel assembled into the magnetic levitation setup. Cellular assembly features were observed *via* microscopy imaging immediately and after the given incubation times. As observed from previous characterization steps, under the given conditions, Gd(III) chelates, especially Gadobutrol, was well tolerated by the cells. 50 mM Gadobutrol (Gadovist), which provided suitable levitation height and good cell viability, was used for 3D cell culture studies. The cells reached the equilibrium height in 1–5 min and aligned at around 425 μm position at 50 mM Gd concentration. Levitating cells at the same equilibrium height facilitated cell–cell interactions while preventing cell attachment to any other solid surface; therefore, cellular assembly and cell proliferation was found to be favored by the magnetic levitation technique. Proliferation behavior of the magnetically levitated cells was compared with that of traditional 2D cell culture (Fig. 5A). An exponential growth was observed for the

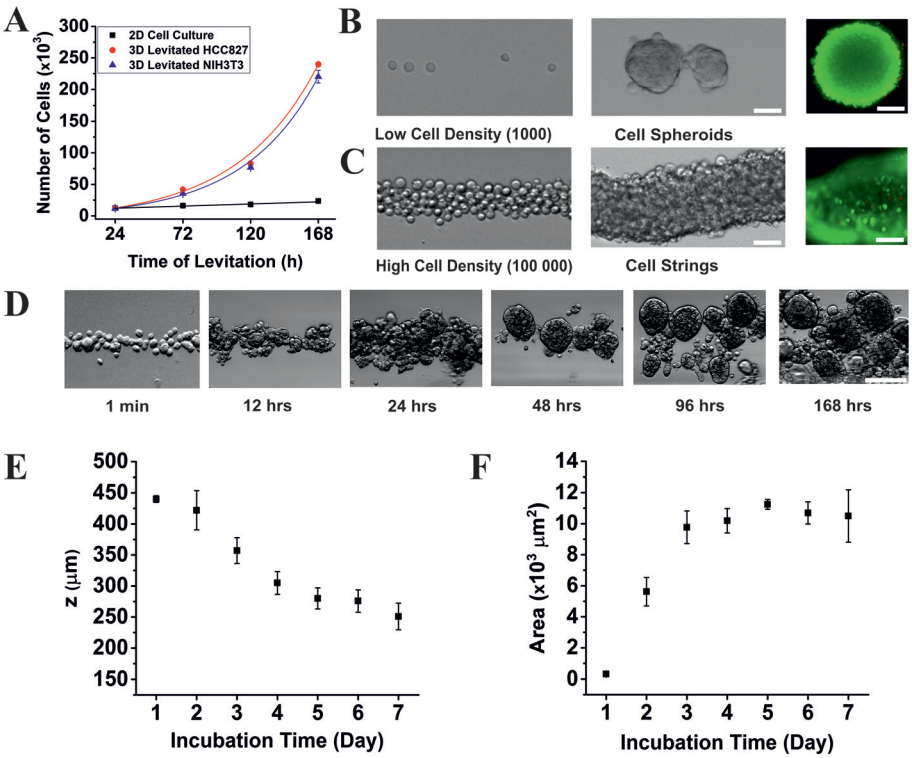

Fig. 5 3D cell culture formation *via* magnetic levitation. (A) Comparison of standard 2D and 3D cell cultures *via* magnetic levitation. Number of cells corresponds to proliferation as a function of incubation time. Following symbols represents the standard 2D cell culture (■), 3D levitated HCC827 culture (●), and 3D levitated NIH 3T3 culture (▲). (B) Formation of 3D cell culture *via* magnetic levitation when low numbers of NIH 3T3 cells were used; aligned cells inside the capillary channel (left), cell spheroid formation (middle), Live/Dead analysis of cell spheroids (right) green: live and red: dead. Scale bar: 50 μm. (C) Formation of 3D cell culture *via* magnetic levitation when high numbers of NIH 3T3 cells were used; aligned cells inside the capillary channel (left), cell string formation (middle), Live/Dead analysis of cell strings (right) green: live and red: dead. Scale bar: 100 μm. (D) Representative time-lapse sequence of light microscope images from 1 min and 12/24/48/96/168 h. (E) Average levitation heights (*z*) of 3D cell cultures for 7 d. (F) Average area values obtained from 3D cell cultures during 7 d.

3D cell culture *via* magnetic levitation, whereas only a linear growth was observed for the standard 2D cell culture. As expected, the magnetic levitation system provided considerable volume for 3D growth, whereas the 2D cell culture environment exhibited limitations in terms of accessible area and volume.

To characterize the cellular assembly *via* magnetic levitation, cell number is varied initially in paramagnetic cell medium. 3D cell culture formation is investigated for a 7 day incubation time. The effect of cell population is demonstrated in Fig. 5B and C for NIH 3T3 cells. The structure and dimensions of the cellular assembly is varied when the cell number is increased. When low numbers of cells (1000) are used, the assembled cells form spheroids (Fig. 5B). However, when high numbers of cells (100 000) are used, they tend to form bigger clusters such as cellular strings (Fig. 5C). The dense cellular interaction triggers the lateral expansion of cell clusters when high numbers of the cells are incubated. It is also considered that whenever the magnetic levitation is applied, all the cells tend to align at the equilibrium height where magnetic and gravitational forces are balanced. Therefore, lateral direction is much more favored than longitudinal direction for cellular growth when high numbers of the cells are used. Magnetic levitation setup is not only good for cellular assembly but also for preserving cell viability during 3D cell culture formation. Cell viabilities of 3D cellular structures are analyzed by Live/Dead analysis, and the results confirm around 99% cell viability in both low number (Fig. 5B) and high number (Fig. 5C) of cells.

Next, to evaluate and quantify the 3D cell culture formation, we microscopically monitored shapes of spheroids, levitation heights and density profiles for 7 days. As given in Fig. 5D, different phases of spheroid formation were monitored with snapshots of a time-lapse sequence. The first image represents the aligned single cells right after insertion into the magnetic levitation setup. After 12 h, individual cells assemble together and aggregate into bigger structures. Later, after 24 h, the cells form more complex and compact 3D clusters. Next, the clusters round up and form individual 3D spheroids in 48 h. It is also observed that single cells or smaller clusters that surround the 3D spheroids increase in size and form new individual spheroids with time, as seen in 96 and 168 h images. Moreover, levitation height profiles (Fig. 5E) and spheroid dimensions in terms of area (Fig. 5F) are evaluated. Levitation

height profiles, which also correspond to density change of the spheroids, reveal that during 7 d incubation, the levitation height of the spheroids gradually decrease up to 250 μm position in the capillary channel. The decreasing levitation height indicates increasing density of the cell spheroids, which is most likely due to an increase in total mass. Additionally, as given in Fig. 5F, the change in dimensions and area exhibits very rapid increase up to 3 d but later slows down. The total mass increases more than the total volume increase; therefore, the density of the cell spheroids increases with time. It can be also anticipated that the cells form very dense and compact structures with ECM formation, which limits the total volume increase; at the same time, the total mass of the spheroids increases due to cell proliferation and ECM secretion.

Conclusion

In conclusion, we have demonstrated the ability of magnetic levitation setup for cellular assembly and 3D cell culture formation without a scaffold or assembling material. Herein, for the first time, we have shown the ability of varied paramagnetic agents, namely, Gd(III) chelates and evaluated their effects on cells and 3D cell culture formation. It is shown that Gadobutrol provides maximum cell viability as compared to other two paramagnetic agents Gadoteric acid and Gadodiamide. Due to the low toxicity of Gadobutrol, intercellular interactions of NIH 3T3 mouse fibroblasts and HCC 827 non-small-cell lung cancer cells have been facilitated *via* magnetic levitation, which induces 3D cell culture formation. These results suggest that the developed magnetic levitation setup is a useful tool for contactless manipulation of cells. It has been also shown that the spheroid characteristics and properties can be tuned easily *via* magnetic levitation. Furthermore, the developed methodology is a simple and easy-to-use method, which does not require complex facilities, devices or chemicals. We foresee that the developed methodology can be applied and the developed setup can be used in varied research areas such as drug screening, tissue engineering and development, regenerative medicine and 3D bioprinting.

Conflicts of interest

There are no conflicts to declare.

Acknowledgements

This study was supported by IYTE BAP; 2016IYTE70. AAY would like to acknowledge UNESCO-Loreal International Fellowship 2014 for their support. We would like to acknowledge Izmir Institute of Technology, Biotechnology and Bioengineering Research and Application Center for the microscopy facilities. We also would like to thank Dr Umit Hakan Yildiz for his feedback on the manuscript.

References

1 K.-H. Nam, A. S. Smith, S. Lone, S. Kwon and D.-H. Kim, *J. Lab. Autom.*, 2015, **20**, 201–215.
2 V. S. Nirmalanandhan, A. Duren, P. Hendricks, G. Vielhauer and G. S. Sittampalam, *Assay Drug Dev. Technol.*, 2010, **8**, 581–590.
3 L. A. Kunz-Schughart, J. P. Freyer, F. Hofstaedter and R. Ebner, *J. Biomol. Screening*, 2004, **9**, 273–285.
4 Y. Fan, D. T. Nguyen, Y. Akay, F. Xu and M. Akay, *Sci. Rep.*, 2016, **6**, 25062.
5 Y. Zhu, K. Kekalo, C. Ndong, Y.-Y. Huang, F. Shubitidze, K. E. Griswold, I. Baker and J. X. J. Zhang, *Adv. Funct. Mater.*, 2016, **26**, 3953–3972.
6 C. R. Thoma, M. Zimmermann, I. Agarkova, J. M. Kelm and W. Krek, *Adv. Drug Delivery Rev.*, 2014, **69–70**, 29–41.
7 C. J. Lovitt, T. B. Shelper and V. M. Avery, *Biology*, 2014, **3**, 345–367.
8 K. Qiu, C. He, W. Feng, W. Wang, X. Zhou, Z. Yin, L. Chen, H. Wang and X. Mo, *J. Mater. Chem. B*, 2013, **1**, 4601–4611.
9 N. D. Shapiro, S. Soh, K. A. Mirica and G. M. Whitesides, *Anal. Chem.*, 2012, **84**, 6166–6172.
10 N. D. Shapiro, K. A. Mirica, S. Soh, S. T. Phillips, O. Taran, C. R. Mace, S. S. Shevkoplyas and G. M. Whitesides, *J. Am. Chem. Soc.*, 2012, **134**, 5637–5646.
11 P. A. Kenny, G. Y. Lee, C. A. Myers, R. M. Neve, J. R. Semeiks, P. T. Spellman, K. Lorenz, E. H. Lee, M. H. Barcellos-Hoff, O. W. Petersen, J. W. Gray and M. J. Bissell, *Mol. Oncol.*, 2007, **1**, 84–96.
12 G. R. Souza, J. R. Molina, R. M. Raphael, M. G. Ozawa, D. J. Stark, C. S. Levin, L. F. Bronk, J. S. Ananta, J. Mandelin, M. M. Georgescu, J. A. Bankson, J. G. Gelovani, T. C. Killian, W. Arap and R. Pasqualini, *Nat. Nanotechnol.*, 2010, **5**, 291–296.
13 S. V. Murphy and A. Atala, *Nat. Biotechnol.*, 2014, **32**, 773–785.
14 A. Arslan-Yildiz, R. El Assal, P. Chen, S. Guven, F. Inci and U. Demirci, *Biofabrication*, 2016, **8**, 014103.
15 H. Akiyama, A. Ito, Y. Kawabe and M. Kamihira, *Biomed. Microdevices*, 2009, **11**, 713–721.
16 A. Akkouch, Z. Zhang and M. Rouabhia, *J. Biomater. Appl.*, 2014, **28**, 922–936.
17 E. W. Young and D. J. Beebe, *Chem. Soc. Rev.*, 2010, **39**, 1036–1048.
18 T. Okuyama, H. Yamazoe, N. Mochizuki, A. Khademhosseini, H. Suzuki and J. Fukuda, *J. Biosci. Bioeng.*, 2010, **110**, 572–576.
19 S. R. Peyton, P. D. Kim, C. M. Ghajar, D. Seliktar and A. J. Putnam, *Biomaterials*, 2008, **29**, 2597–2607.
20 A. Atala, *J. Tissue Eng. Regener. Med.*, 2007, **1**, 83–96.
21 L. Almany and D. Seliktar, *Biomaterials*, 2005, **26**, 2467–2477.
22 H. Tseng, J. A. Gage, R. M. Raphael, R. H. Moore, T. C. Killian, K. J. Grande-Allen and G. R. Souza, *Tissue Eng., Part C*, 2013, **19**, 665–675.

23 L. G. Griffith and M. A. Swartz, *Nat. Rev. Mol. Cell Biol.*, 2006, **7**, 211–224.
24 E. L. S. Fong, S.-E. Lamhamedi-Cherradi, E. Burdett, V. Ramamoorthy, A. J. Lazar, F. K. Kasper, M. C. Farach-Carson, D. Vishwamitra, E. G. Demicco and B. A. Menegaz, *Proc. Natl. Acad. Sci. U. S. A.*, 2013, **110**, 6500–6505.
25 M. E. Hoque, T. T. H. Meng, Y. L. Chuan, M. Chowdhury and R. G. S. V. Prasad, *Mater. Lett.*, 2014, **131**, 255–258.
26 Y. Sharma, A. Tiwari, S. Hattori, D. Terada, A. K. Sharma, M. Ramalingam and H. Kobayashi, *Int. J. Biol. Macromol.*, 2012, **51**, 627–631.
27 M. Younesi, V. M. Goldberg and O. Akkus, *Acta Biomater.*, 2016, **30**, 212–221.
28 J. Arulmoli, H. J. Wright, D. T. T. Phan, U. Sheth, R. A. Que, G. A. Botten, M. Keating, E. L. Botvinick, M. M. Pathak, T. I. Zarembinski, D. S. Yanni, O. V. Razorenova, C. C. W. Hughes and L. A. Flanagan, *Acta Biomater.*, 2016, **43**, 122–138.
29 P. B. Malafaya, G. A. Silva and R. L. Reis, *Adv. Drug Delivery Rev.*, 2007, **59**, 207–233.
30 C. B. Hutson, J. W. Nichol, H. Aubin, H. Bae, S. Yamanlar, S. Al-Haque, S. T. Koshy and A. Khademhosseini, *Tissue Eng., Part A*, 2011, **17**, 1713–1723.
31 J. W. Nichol, S. T. Koshy, H. Bae, C. M. Hwang, S. Yamanlar and A. Khademhosseini, *Biomaterials*, 2010, **31**, 5536–5544.
32 V. M. Merkle, P. L. Tran, M. Hutchinson, K. R. Ammann, K. DeCook, X. Wu and M. J. Slepian, *Acta Biomater.*, 2015, **27**, 77–87.
33 D. J. Choi, S. M. Choi, H. Y. Kang, H. J. Min, R. Lee, M. Ikram, F. Subhan, S. W. Jin, Y. H. Jeong, J. Y. Kwak and S. Yoon, *J. Biotechnol.*, 2015, **205**, 47–58.
34 A. K. Ekaputra, G. D. Prestwich, S. M. Cool and D. W. Hutmacher, *Biomaterials*, 2011, **32**, 8108–8117.
35 W. L. Haisler, D. M. Timm, J. A. Gage, H. Tseng, T. C. Killian and G. R. Souza, *Nat. Protoc.*, 2013, **8**, 1940–1949.
36 O. Frey, P. M. Misun, D. A. Fluri, J. G. Hengstler and A. Hierlemann, *Nat. Commun.*, 2014, **5**, 4250.
37 E. Rosines, K. Johkura, X. Zhang, H. J. Schmidt, M. Decambre, K. T. Bush and S. K. Nigam, *Tissue Eng., Part A*, 2010, **16**, 2441–2455.
38 V. H. Ho, K. H. Muller, A. Barcza, R. Chen and N. K. Slater, *Biomaterials*, 2010, **31**, 3095–3102.
39 S. Tasoglu, C. H. Yu, V. Liaudanskaya, S. Guven, C. Migliaresi and U. Demirci, *Adv. Healthcare Mater.*, 2015, **4**, 1469–1476.
40 S. Tasoglu, J. A. Khoory, H. C. Tekin, C. Thomas, A. E. Karnoub, I. C. Ghiran and U. Demirci, *Adv. Mater.*, 2015, **27**, 3901–3908.
41 M. R. Dzamukova, E. A. Naumenko, E. V. Rozhina, A. A. Trifonov and R. F. Fakhrullin, *Nano Res.*, 2015, **8**, 2515–2532.
42 L. Rodriguez-Arco, I. A. Rodriguez, V. Carriel, A. B. Bonhome-Espinosa, F. Campos, P. Kuzhir, J. D. Duran and M. T. Lopez-Lopez, *Nanoscale*, 2016, **8**, 8138–8150.
43 N. G. Durmus, H. C. Tekin, S. Guven, K. Sridhar, A. Arslan Yildiz, G. Calibasi, I. Ghiran, R. W. Davis, L. M. Steinmetz and U. Demirci, *Proc. Natl. Acad. Sci. U. S. A.*, 2015, **112**, E3661–E3668.
44 A. Huppertz and M. Rohrer, *Eur. Radiol.*, 2004, **14**, M12–M18.
45 D. A. Stojanov, A. Aracki-Trenkic, S. Vojinovic, D. Benedeto-Stojanov and S. Ljubisavljevic, *Eur. Radiol.*, 2016, **26**, 807–815.
46 J. M. Idee, M. Port, C. Medina, E. Lancelot, E. Fayoux, S. Ballet and C. Corot, *Toxicology*, 2008, **248**, 77–88.